高等学校化学学报
CHEMICAL JOURNAL OF CHINESE UNIVERSITIES
研究论文

甲酸-草酸共配体低维磁性镱配合物的构筑及磁性

翟晓璐[1]，吕　云[1]，李　会[1]，黄科科[2]，王艳红[1]，卢红成[1,3]

（1. 华中科技大学化学与化工学院，能量转换与存储材料化学教育部重点实验室，
材料化学与服役失效湖北省重点实验室，武汉 430074；
2. 无机合成与制备化学全国重点实验室，吉林大学化学学院，长春 130012；
3. 华中科技大学国家脉冲强磁场科学中心，武汉 430074）

摘要　采用溶剂热法合成了一例新型层状磁性镱配合物Yb(HCOO)(C_2O_4)(1,10-phen)(1,10-phen=邻菲罗啉)；利用X射线衍射(XRD)、红外光谱(IR)、热重分析(TGA)和磁化率测试等手段对其晶体结构和磁性进行了表征．单晶结构分析表明，该配合物中磁性离子Yb^{3+}通过甲酸根与草酸根连接形成四方磁晶格层，层间通过邻菲罗啉配体隔开．磁性测试结果显示，配合物中Yb^{3+}间以反铁磁相互作用占主导，且在温度低至2 K时未出现长程磁有序．本研究为构筑具有低维磁性的稀土配合物提供了新的合成策略．

关键词　低维磁性；晶体结构；镱配合物；溶剂热法

中图分类号　O614　　**文献标志码**　A　　doi：10.7503/cjcu20260193

Construction and Magnetic Properties of Low-dimensional Ytterbium(III) Coordination Polymers Based on Formate and Oxalate Co-Ligands

ZHAI Xiaolu[1], LV Yun[1], LI Hui[1], HUANG Keke[2], WANG Yanhong[1*], LU Hongcheng[1,3*]

(*1. School of Chemistry and Chemical Engineering, Key Laboratory of Material Chemistry for Energy Conversion and Storage, Ministry of Education, Hubei Key Laboratory of Materials Chemistry and Service Failure, Huazhong University of Science and Technology, Wuhan* 430074, *China*;
2. State Key Laboratory of Inorganic Synthesis and Preparative Chemistry, College of Chemistry, Jilin University, Changchun 130012, *China*;
3. Wuhan National High Magnetic Field Center, Huazhong University of Science and Technology, Wuhan 430074, *China*)

Abstract　A novel layered magnetic ytterbium coordination compound, Yb(HCOO)(C_2O_4)(1,10-phen)(1,10-phen=1,10-phenanthroline), was synthesized *via* a solvothermal method. Its crystal structure and magnetic properties were characterized by means of X-ray diffraction(XRD), infrared spectroscopy(IR), thermogravimetric analysis(TGA), and magnetic susceptibility measurements. Single-crystal structure analysis reveals that the magnetic Yb^{3+} ions are connected by formate and oxalate ligands to form a square magnetic lattice, with adjacent layers separated by 1,10-phen

收稿日期：2026-05-10. 网络首发日期：2026-05-31.
联系人简介：王艳红，女，博士，主要从事有机-无机杂化低维量子磁性材料方面的研究．E-mail: yhw1006@hust.edu.cn
卢红成，男，博士，教授，主要从事基于自旋电子器件和量子计算/存储应用的光电磁功能晶体材料方面的研究．E-mail: hcl@hust.edu.cn
基金项目：国家自然科学基金(批准号：22422111)资助．
Supported by the National Natural Science Foundation of China(No.22422111).

ligands. Magnetic measurements show that the dominant interaction between the Yb^{3+} ions is antiferromagnetic, and no long-range magnetic order is observed down to 2 K. This study provides a new synthetic strategy for constructing low-dimensional magnetic rare-earth coordination compounds.

Keywords Low-dimensional magnetism; Crystal structure; Ytterbium coordination compound; Solvothermal method

1 Introduction

Lanthanide-based magnetic materials have garnered considerable interest because of their unique 4*f* electronic configurations, strong spin-orbit coupling, and intriguing magnetic phenomena, such as single-molecule magnetism, magnetocaloric effect, and quantum spin liquid state, which are of potential applications in spintronic devices, high-density information storage, and quantum computing[1~9]. Among them, the research on two-dimensional lanthanide-based antiferromagnets is extremely active due to their exotic quantum magnetism. For example, lanthanide-based magnetic materials with the triangular lattice, such as $YbMgGaO_4$ and the family compounds $ARECh_2$ (alkali or monovalent ions, RE=rare earth, Ch=O, S, Se), have been proposed as quantum spin liquid candidates[7,10]. A magnetic field-tuned anisotropic quantum phase transition has been observed in the antiferromagnet Nd_3BWO_9 with a distorted kagome lattice[11]. Thus, designing more two-dimensional lanthanide-based magnetic materials is crucial to exploring other interesting magnetic behaviors.

Up to now, synthetic chemists have utilized single or mixed basic building units to experimentally design and synthesize various low-dimensional lanthanide-based antiferromagnets, such as single ions of O^{2-}[7,12], S^{2-}[10,13], Se^{2-}[10,14], Te^{2-}[15], and inorganic groups of BO_3^{3-}[16,17], VO_4^{3-}[18], SO_4^{2-}[19], PO_4^{3-}[20]. Furthermore, the use of small organic bridging ligands, including formate ($HCOO^-$) and oxalate ($C_2O_4^{2-}$), to construct low-dimensional lanthanide-based coordination polymers has attracted increasing attention as they can create some interesting materials[5,21~23]. Gadolinium-oxalate framework $Gd_2(C_2O_4)_3(H_2O)_6\cdot(0.6H_2O)$ with honeycomb lattice exhibits good magnetocaloric effect[5]. Oxalatophosphonate $[Dy_2(H_3L)(C_2O_4)_3(H_2O)_4]\cdot 2H_2O$ [H_3L=(4-carboxypiperidyl)-*N*-methylenephosphonic acid] with a layered structure shows antiferromagnetic interactions between the Dy^{3+} ions[21]. Although low-dimensional lanthanide-based magnetic materials coordinated with formate or oxalate ligands have been extensively reported, lanthanide-based coordination compounds with mixed formate and oxalate co-ligands are still very limited[24~27].

In this work, a new ytterbium coordination compound Yb(HCOO)(C_2O_4)(1,10-phen)(1,10-phen=1,10-phenanthroline) with a two-dimensional square lattice has been successfully synthesized based on formate and oxalate co-ligands. Magnetic susceptibility results indicate dominant antiferromagnetic exchange interactions and the absence of long-range order down to 2 K. Attenuated total reflectance-Fourier transform infrared spectrum and thermal stability are also reported.

2 Experimental

2.1 Reagents and Instruments

Ytterbium (III) chloride hexahydrate ($YbCl_3\cdot 6H_2O$, A. R., 99.99%, Shanghai Aladdin Biochemical Technology Co., Ltd.), oxalic acid dihydrate ($H_2C_2O_4\cdot 2H_2O$, A. R., 99%, Sinopharm Chemical Reagent Co., Ltd.), 1,10-phenanthroline (1,10-phen, R. G., 99%, Adamas, Titan Scientific Co., Ltd.) and *N*,*N*-dimethylformamide (DMF, 99.5%, Shanghai Aladdin Biochemical Technology Co., Ltd.) were used as received without further purification.

Powder X-ray diffraction (PXRD) pattern was collected at room temperature on a SmartLab SE powder X-ray diffractometer (Rigaku, Japan) with Cu *Kα* radiation (λ=0.154184 nm). The attenuated total reflectance-Fourier

transform infrared(ATR-FTIR) spectrum was recorded using a Vertex 70 FTIR spectrometer(Bruker, Germany) in the range of 400—4000 cm^{-1}. Thermogravimetric analysis(TGA) was conducted on a Diamond TG/DTA thermal analyzer instrument(PerkinElmer Instruments, China), heating to 885 ℃ with a heating rate of 10 ℃/min in a N_2 atmosphere. The powder sample for magnetic measurements was prepared by grinding small single crystals. DC magnetic susceptibility measurements were performed on MPMS3 superconducting quantum interference device magnetometer(Quantum Design, USA) between 2 K and 300 K with an applied field of 0.1 T. The field-dependent magnetization was measured at 2 K in an applied field from −7 T to +7 T. The diamagnetic contribution was subtracted by using Pascal's constants[28].

2.2 Synthesis of Yb(HCOO)(C_2O_4)(1,10-phen)

A mixture of $YbCl_3·6H_2O$(0.1162 g, 0.3 mmol), $H_2C_2O_4·2H_2O$(0.0378 g, 0.3 mmol), and 1,10-phen (0.0541 g, 0.3 mmol) was sealed in a 25 mL Teflon-lined stainless steel autoclave with deionized water (2 mL) and DMF(1 mL). The mixture was quickly heated to 140 ℃, held at this temperature for 72 h, and cooled slowly to room temperature for 33 h. Light yellow crystals of Yb(HCOO)(C_2O_4)(1,10-phen) were collected by washing with deionized water.

2.3 Crystallographic Determination

A suitable single crystal of Yb(HCOO)(C_2O_4)(1,10-phen) was carefully selected and mounted on a loop ring for single-crystal X-ray diffraction measurement. Diffraction data were collected at 298 K using a XtaLAB mini II two-circle diffractometer(Rigaku, Japan) equipped with a monochromated Mo $K\alpha$ radiation (λ = 0.071073 nm), then run by the program CrysAlisPro. The multi-scan method was used for correcting all the reflection intensities. The structure was solved by the intrinsic phasing method in SHELXT[29] and subsequently refined by the least-squares method based on SHELXL[30] within Olex 2 software[31]. All non-hydrogen atoms were refined with anisotropic thermal parameters. The hydrogen atoms were placed in calculated positions and refined isotropically. And the final refined structure was checked using the PLATON program[32], and no higher symmetry was found. Crystallographic parameters and structural refinement were summarized in Table 1.

Table 1 Crystal data and structural refinements for Yb(HCOO)(C_2O_4)(1,10-phen)

Compound formula	$YbC_{15}H_9N_2O_6$	V/nm^3	1.44461(5)
Formula weight/(g·mol^{-1})	486.28	Z	4
Temperature/K	298	Maximum θ/(°)	30.025
Crystal system	Monoclinic	λ(Mo $K\alpha$)/nm	0.071073
Space group	$P2_1/c$	$\rho_{calc.}$/(g·cm^{-3})	2.236
a/nm	0.64006(1)	μ/mm^{-1}	6.510
b/nm	1.98162(5)	R_{int}	0.0338
c/nm	1.21616(3)	Final R indexes[I >= 2σ(I)]*	R_1=0.0259, wR_2=0.0516
α/(°)	90	Final R indexes[all data]	R_1=0.0339, wR_2=0.0539
β/(°)	110.524(2)	Goodness-of-fit on F^2	1.044
γ/(°)	90		

* $R_1=\sum||F_o|-|F_c||/\sum|F_o|$, $wR_2=\{\sum w[(F_o)^2-(F_c)^2]^2/\sum w[(F_o)^2]^2\}^{1/2}$.

3 Results and Discussions

3.1 Structural Description

The phase purity for Yb(HCOO)(C_2O_4)(1,10-phen) was confirmed by the powder X-ray diffraction (Fig. S1, see the supporting information of this paper). Single-crystal X-ray diffraction analysis shows that Yb(HCOO)(C_2O_4)(1,10-phen) crystallizes in the monoclinic space group $P2_1/c$ with a=0.64006(1) nm, b=1.98162(5) nm, c=1.21616(3) nm, $\alpha=\gamma=90°$, and β=110.524(2)°. There is one ytterbium ion, one formate anion, halves of two different oxalate anions, and one 1,10-phen ligand in an asymmetric unit. As

shown in Fig.1(A), Yb(HCOO)(C_2O_4)(1,10-phen) is a two-dimensional layered structure with the 1,10-phen ligand filling the interlayer along the *b* axis. Adjacent layers connect with each other *via* weak hydrogen bonds(C—H···O)(Table S1 in the supporting information of this paper) to stabilize the crystal structure of Yb(HCOO)(C_2O_4)(1,10-phen). The shortest interlayer Yb···Yb distance is 1.01672(5) nm. Within each layer, the adjacent Yb^{3+} ions are connected by formate groups along the *a* axis with a distance of 0.64006(2) nm. Along the *c* axis, the adjacent Yb^{3+} ions are connected by oxalate groups with the distances of 0.60387(4) nm and 0.60855(4) nm[Fig.1(B) and (C)]. Consequently, Yb^{3+} ions form a square spin lattice. Each Yb^{3+} ion is eight-coordinated with two nitrogen atoms(Yb—N=0.2489(3)—0.2506(3) nm) from one 1,10-phen ligand and six oxygen atoms(Yb—O=0.2223(2)—0.2382(2) nm) from two formate groups and two oxalate groups [Fig.1(D)]. Bond valence sum(BVS) calculations[33] show that the oxidation state of Yb is +3(Table S2 in the Supporting Information of this paper).

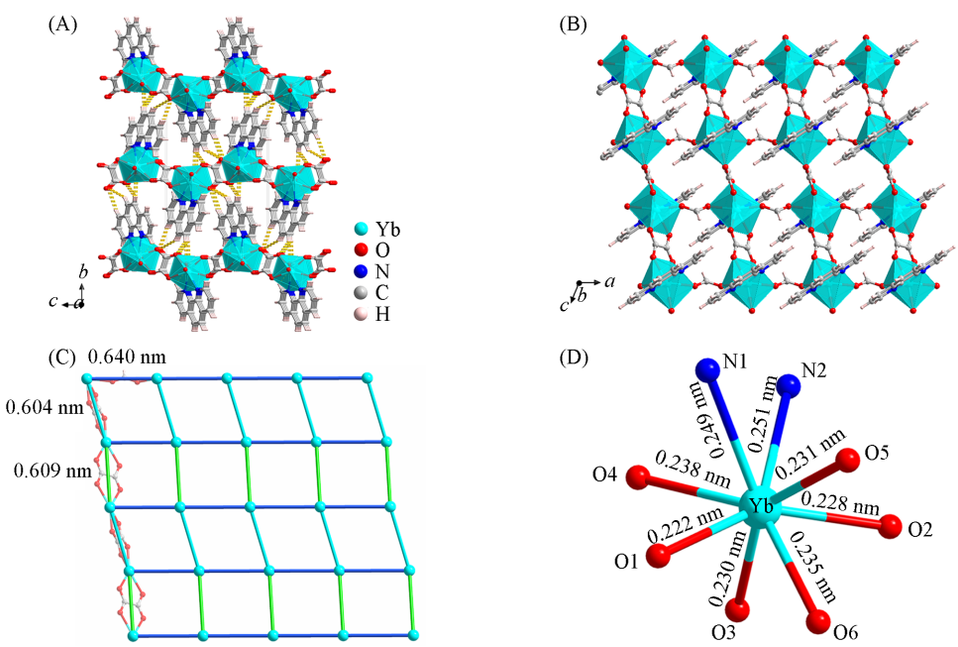


Fig. 1 Crystal structure of Yb(HCOO)(C_2O_4)(1,10-phen)

(A) Layers stacking along the *b* axis; (B) the layer of Yb(HCOO)(C_2O_4)(1,10-phen) in the *ac* plane; (C) square spin lattice of Yb^{3+} ions; (D) local coordination environment of Yb^{3+} ion.

3.2 ATR-FTIR Spectrum

The ATR-FTIR spectrum for Yb(HCOO)(C_2O_4)(1,10-phen) is presented in Fig.2. The adsorption band at 2845 cm^{-1} is assigned to ν(C—H). The characteristic bands of formate and oxalate ligands can be observed at 1679, 1632, 1356, 1313, 1136 and 1096 cm^{-1} due to the ν_{as}(C═O), ν_s(C═O) and ν_s(C—O)[34]. The adsorption band at 797 cm^{-1} belongs to the bending vibration of δ(O—C═O)[34]. The bands in the range of 866—640 cm^{-1} are attributed to the out-of-plane bending vibrations of the C—H bonds on the aromatic ring of 1,10-phen. In addition, the bands at *ca.* 488 cm^{-1} and *ca.* 415 cm^{-1} are correspond to ν(Yb—N) and ν(Yb—O) vibrations[35,36].

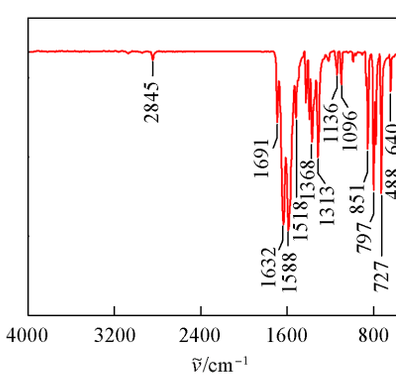


Fig. 2 ATR-FTIR spectrum for Yb(HCOO)(C_2O_4)·(1,10-phen)

3.3 Thermal analysis

To investigate the thermal stability of Yb(HCOO)(C_2O_4)(1,10-phen), thermogravimetric measurement was performed, as shown in Fig. 3. It can be seen that Yb(HCOO)(C_2O_4)(1,10-phen) remained stable up to 300 ℃ and then showed a two-step mass loss up to 885 ℃. The first loss between 300 ℃ and 450 ℃ is assigned to the decomposition of formate and 1,10-phen ligands (observed: 43.03%; expected: 46.32%). The second loss, which is continuous up to 885 ℃, corresponds to the decomposition of oxalate ligands (observed: 14.22%; expected: 18.10%). The observed total mass loss of 57.25% is slightly less than the expected value of 59.48% (assuming the final residue corresponds to Yb_2O_3), which may be due to incomplete decomposition.

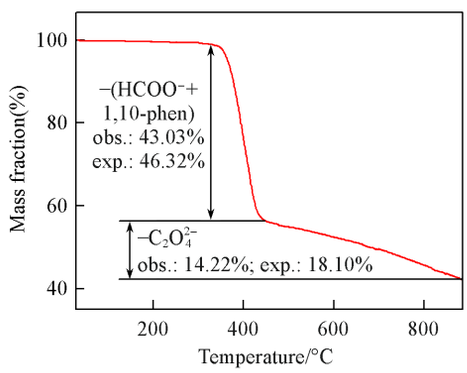


Fig. 3 TGA curve for Yb(HCOO)(C_2O_4)(1,10-phen)

3.4 Magnetic Property

Fig.4(A) illustrates the zero-field cooling(ZFC) and field cooling(FC) magnetic susceptibility(χ=M/H) for Yb(HCOO)(C_2O_4)(1,10-phen) measured at 0.1 T between 2 K and 300 K. The magnetic susceptibility increases with decreasing temperature, and no sharp λ-shape peak is observed, indicating no magnetic long-range order occurred down to 2 K. Also, there is no divergence between the ZFC and FC curves, ruling out the possibility of spin glass and spin canting behaviors. Then, a Curie-Weiss law of χ=C/(T − θ) is applied to fit the inverse susceptibility χ^{-1}(T), where the parameters C and θ are the Curie constant and the Curie-Weiss temperature, respectively. As shown in Fig.4(B), the high temperature (200—300 K) Curie-Weiss fit yields a negative Curie-Weiss temperature (θ_{HT}) of −47.18(20) K and an effective magnetic moment μ_{eff}(HT) of 4.56(1) μ_B, which is in good agreement with the expected value (4.54 μ_B) for a free Yb^{3+} ion (J=7/2, g=8/7). Since a high-temperature Curie-Weiss fit of θ includes contributions from thermally populated crystal field levels, the large value of θ_{HT} does not originate from the magnetic exchange interaction but results from this thermal modification effect on the Yb^{3+} ion[18,37,38]. In the low-temperature region from 2 K to 10 K, the Curie-Weiss fit gives a negative θ_{LT} of −0.31(1) K and μ_{eff}(LT) of 3.02(1) μ_B. The negative Curie-Weiss temperature indicates dominant antiferromagnetic interactions between the Yb^{3+} ions. The low-temperature magnetic behavior of Yb(HCOO)(C_2O_4)(1,10-phen) is due to an effective spin J_{eff}=1/2 ground state of the Yb^{3+} ion. The smaller effective magnetic moment is close to the other reported Yb^{3+}-based

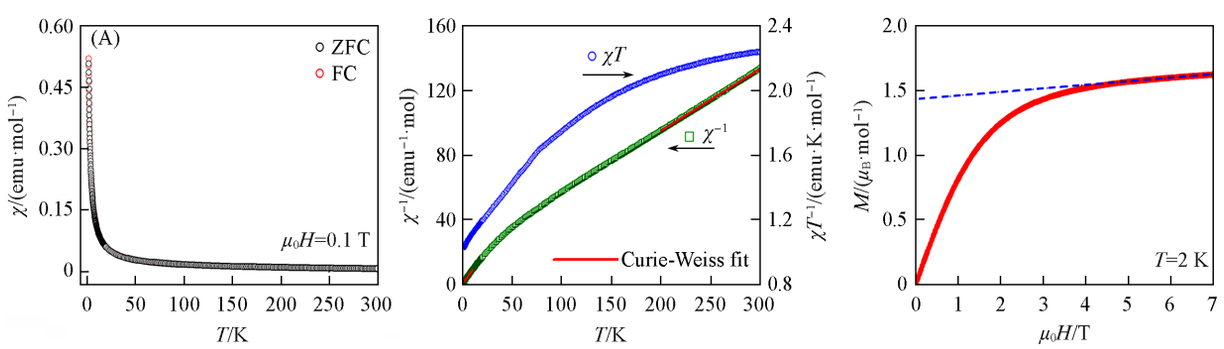


Fig. 4 ZFC(black) and FC(red) magnetic susceptibility for Yb(HCOO)(C_2O_4)(1,10-phen) measured at 0.1 T(A), χ^{-1}–T(green), χT–T(blue) and Curie-Weiss fit(red) curves(B), and field-dependent magnetization measured at 2 K(C)

(C) Blue dashed line: van Vleck contribution. 1 emu = 10^{-3} A·m^2.

systems such as $KYb_2F_5SO_4$[37], $AYbCh_2$(A=Na, K, Rb; Ch=S, Se, O)[12,39,40]. And it also indicates that the Yb^{3+} ion is already in a Kramer's doublet state. The χT value decreases as the temperature decreases, which can be attributed to the gradual depopulation of crystal-field excited states, leading to a reduction in the effective magnetic moment for Yb(HCOO)(C_2O_4)(1,10-phen). The isothermal magnetization was measured between −7 T and 7 T at 2 K as shown in Fig.4(C) and Fig.S2(see the supporting information of this paper). No magnetic hysteresis is observed between −7 T and 7 T, which agrees with antiferromagnetic interactions in Yb(HCOO)(C_2O_4)(1,10-phen). The magnetization curve increases rapidly up to 3 T, and then continues to increase linearly slowly up to 7 T with a small slope, which can be attributed to the Van Vleck contribution. The saturated moment is *ca*. 1.433(1) μ_B after subtracting the Van Vleck contribution [χ_{vv}=0.0151(1) emu/mol, 1 emu=10^{-3} A·m^2] determined from the linear slope above 5 T, which is comparable to those of other Yb^{3+} compounds, including $NaYbO_2$[12,20,37]. The small magnetization further supports the formation of doublet ground states of the Yb^{3+} ion with J_{eff}=1/2.

4 Conclusions

In conclusion, a new hybrid Yb(III)-based layered magnetic compound Yb(HCOO)(C_2O_4)(1,10-phen) was constructed by combining the formate and oxalate ligands. Magnetic measurements indicate that Yb(HCOO)(C_2O_4)(1,10-phen) displays a dominant antiferromagnetic exchange interaction between the Yb^{3+} ions without a magnetic long-range order down to 2 K. Overall, this work provides an effective approach with the combination of formate and oxalate as co-ligands for constructing low-dimensional magnetic rare-earth coordination compounds.

The supporting information of this paper see http://www.cjcu.jlu.edu.cn/CN/10.7503/cjcu20260193.

CCDC Number 2523375 contains the full crystallographic data of Yb(HCOO)(C_2O_4)(1,10-phen).

References

[1] Wang Y. X., Su D., Ma Y., Sun Y., Cheng P., *Nat. Commun.*, **2023**, *14*(1), 7901
[2] Xu W. J., Luo Q. C., Fang Y., Yuan C. J., Lu J. T., Zhai Y. Q., Wang Y., Zheng Y. Z., *Chinese Chem. Lett.*, **2026**, *37*(7), 110975
[3] Wu J., Zhu Z., Tang J., *Chinese Chem. Lett.*, **2025**, *36*(12), 110577
[4] Kitchen J. A., *Coord. Chem. Rev.*, **2017**, *340*, 232—246
[5] Sibille R., Didelot E., Mazet T., Malaman B., François M., *APL Mater.*, **2014**, *2*(12), 124402
[6] Wang M., Meng X., Liu N., Zhang Y. Q., Xu N., Shi W., Cheng P., *Chinese Chem. Lett.*, **2023**, *34*(6), 107995
[7] Li Y., Liao H., Zhang Z., Li S., Jin F., Ling L., Zhang L., Zou Y., Pi L., Yang Z., Wang J., Wu Z., Zhang Q., *Sci. Rep.*, **2015**, *5*(1), 16419
[8] Zhang L., Xiong J., Meng Y. S., Liu T., *Chinese Chem. Lett.*, **2023**, *34*(8), 108055
[9] Zou Q., Liu J. C., Huang X. D., Bao S. S., Zheng L. M., *Chinese Chem. Lett.*, **2021**, *32*(4), 1519—1522
[10] Liu W., Zhang Z., Ji J., Liu Y., Li J., Wang X., Lei H., Chen G., Zhang Q., *Chinese Phys. Lett.*, **2018**, *35*(11), 117501
[11] Song F., Ge H., Liu A., Qin Y., Han Y., Ling L., Yuan S., Ouyang Z., Sheng J., Wu L., Tian Z., *Phys. Rev. B*, **2023**, *108*(21), 214410
[12] Ranjith K. M., Dmytriieva D., Khim S., Sichelschmidt J., Luther S., Ehlers D., Yasuoka H., Wosnitza J., Tsirlin A. A., Kühne H., Baenitz M., *Phys. Rev. B*, **2019**, *99*(18), 180401
[13] Gao S., Xiao F., Kamazawa K., Ikeuchi K., Biner D., Krämer K. W., Rüegg C., Arima T., *Phys. Rev. B*, **2020**, *102*(2), 024424
[14] Xing J., Sanjeewa L. D., Kim J., Stewart G. R., Du M. H., Reboredo F. A., Custelcean R., Sefat A. S., *ACS Mater. Lett.*, **2020**, *2*(1), 71—75
[15] Liu W., Zhang Z., Yan D., Li J., Zhang Z., Ji J., Jin F., Shi Y., Zhang Q., *Chinese Phys. Lett.*, **2024**, *41*(9), 097503
[16] Lv Y., Wang Y., Shi N., Huang K., Tang J., Lu H., *Dalton Trans.*, **2026**, *55*(9), 3786—3794
[17] Xia M., Zhai K., Lu J., Sun Y., Li R. K., *Inorg. Chem.*, **2017**, *56*(14), 8100—8105
[18] Voma U. K., Bhattacharya S., Kermarrec E., Alam J., Jana Y. M., Sana B., Khuntia P., Panda S. K., Koteswararao B., *Phys. Rev. B*, **2021**, *104*(14), 144411

[19] Liu L., Meng H., Li G., Cui Y., Wang X., Pang W., *J. Solid State Chem.*, **2005**, *178*(4), 1003—1007
[20] Guo S., Zhong R., Górnicka K., Klimczuk T., Cava R. J., *Chem. Mater.*, **2020**, *32*(24), 10670—10677
[21] Wang T. T., Su Y. M., Jiao C. Q., Cai X. O., Sun H. M., Zhu Y. Y., Sun Z. G., *New J. Chem.*, **2018**, *42*(2), 1235—1242
[22] Zhang X., Xing Y., Wang C., Han J., Li J., Ge M., Zeng X., Niu S., *Inorg. Chim. Acta*, **2009**, *362*(4), 1058—1064
[23] Lorusso G., Sharples J. W., Palacios E., Roubeau O., Brechin E. K., Sessoli R., Rossin A., Tuna F., McInnes E. J. L., Collison D., Evangelisti M., *Adv. Mater.*, **2013**, *25*(33), 4653—4656
[24] Falsaperna M., Stenning G. B. G., Silva I., Saines P. J., *J. Mater. Chem. C*, **2021**, *9*(38), 13209—13217
[25] Hitchings T. J., Scatena R., Allan D. R., Cairns A. B., Saines P. J., *Chem. Commun.*, **2024**, *60*(24), 3271—3274
[26] Burley L. G., Srivastava A. K., Rudić S., Saines P. J., *Eur. J. Inorg. Chem.*, **2021**, *2021*(37), 3806—3811
[27] Romero S., Mosset A., Trombe J. C., *J. Solid State Chem.*, **1996**, *127*(2), 256—266
[28] Bain G. A., Berry J. F., *J. Chem. Educ.*, **2008**, *85*(4), 532
[29] Sheldrick G. M., *Acta Crystallogr. Sect. A*: *Found. Crystallogr.*, **2015**, *71*(1), 3—8
[30] Sheldrick G. M., *Acta Crystallogr. Sect. C*: *Struct. Chem.*, **2015**, *71*(1), 3—8
[31] Dolomanov O. V., Bourhis L. J., Gildea R. J., Howard J. A. K., Puschmann H., *J. Appl. Crystallogr.*, **2009**, *42*(2), 339—341
[32] Spek A. L., *J. Appl. Crystallogr.*, **2003**, *36*(1), 7—13
[33] Brese N. E., O'Keeffe M., *Acta Crystallogr. Sect. B*: *Struct. Sci.*, **1991**, *47*(2), 192—197
[34] Kang J., Lee Y., Kim S., Yun H., Do J., *Bull. Korean Chem. Soc.*, **2014**, *35*(11), 3244—3248
[35] Lv Y., Wang Y., Dou Y., Li A., Tang J., Volkova O. S., Vasiliev A. N., Lu H., *Cryst. Growth Des.*, **2025**, *25*(8), 2446—2455
[36] Dasari S., Singh S., Kumar P., Sivakumar S., Patra A. K., *Eur. J. Med. Chem.*, **2019**, *163*, 546—559
[37] Jiang N., La Pierre H. S., *Inorg. Chem.*, **2019**, *58*(18), 12152—12156
[38] Mugiraneza S., Hallas A. M., *Commun. Phys.*, **2022**, *5*(1), 95
[39] Baenitz M., Schlender P., Sichelschmidt J., Onykiienko Y. A., Zangeneh Z., Ranjith K. M., Sarkar R., Hozoi L., Walker H. C., Orain J. C., Yasuoka H., Brink J., Klauss H. H., Inosov D. S., Doert T., *Phys. Rev. B*, **2018**, *98*(22), 220409
[40] Xing J., Sanjeewa L. D., May A. F., Sefat A. S., *APL Mater.*, **2021**, *9*(11), 111104

(Ed.: F, K)